Science Translational Medicine

MAAAS

Supplementary Materials for

Impact of antibiotic treatment and host innate immune pressure on enterococcal adaptation in the human bloodstream

Daria Van Tyne, Abigail L. Manson, Mark M. Huycke, John Karanicolas, Ashlee M. Earl, Michael S. Gilmore*

*Corresponding author. Email: michael_gilmore@meei.harvard.edu

The PDF file includes:

Materials and Methods
Fig. S1. Phenotypic differences between pre-outbreak and outbreak *E. faecalis* strains.
Fig. S2. Comparison of *E. faecalis* B594 and V583 strain genomes.
Fig. S3. Phylogeny of 62 *E. faecalis* outbreak strains.
Fig. S4. Summary of gene expression differences between *gntR* wild-type and mutant *E. faecalis* strains measured by RNA sequencing.
Fig. S5. Difference in autolysis between *gntR* wild-type and mutant strains.
Fig. S6. Morphological differences between *gntR* wild-type and mutant strains.
Fig. S7. Growth curves of MMH594 wild-type and mutant strains in the presence of different sugars.
Fig. S8. Active site modeling of the GHF65 enzyme.
Fig. S9. Increased resistance to ampicillin killing in *gntR* mutants due to the constitutive expression of the GHF65 enzyme.
Fig. S10. Killing assay in whole human blood with *pbp4* wild-type and mutant strains.
Fig. S11. Predicted secondary structure of the region upstream of *pbp4* and location of mutations identified in in vitro–selected meropenem-resistant strains.
References (*44–72*)

Other Supplementary Material for this manuscript includes the following:

(available at www.sciencetranslationalmedicine.org/cgi/content/full/11/487/eaat8418/DC1)

Table S1 (Microsoft Excel format). Strain and genome information for analyzed strains.
Table S2 (Microsoft Excel format). Gene enrichment among outbreak lineages.
Table S3 (Microsoft Excel format). Filtered variants detected in 62 outbreak strains.
Table S4 (Microsoft Excel format). Variants detected in outbreak strains isolated from the same patient.
Table S5 (Microsoft Excel format). GntR and PBP4 mutations identified in nonoutbreak strains.

Materials and Methods

Whole-genome sequencing and assembly

PacBio libraries were generated following the manufacturer's recommendations (Procedure & Checklist - 20 kb Template Preparation Using BluePippin Size-Selection v1 and Guidelines for Preparing Size-Selected ~20kb SMRTbell Templates v1), using the DNA Template Prep Kit 2.0 (3Kb - 10Kb) with the following modifications: For each sample, 10 ug of genomic DNA was sheared using Covaris G-tubes at 4800 RPMs. Due to the low shearing size, DNA fragments were purified, DNA damage was end-repaired, and fragments were ligated with SMRTbell sequencing adapters following the manufacturer's recommendations (Procedure & Checklist - 2 kb Template Preparation and Sequencing v13). SMRTbell sequencing libraries were combined with sequencing primer and polymerase using DNA/Polymerase Binding Kit 2.0 and v2.0.1.2 Sample Prep Calculator. The resulting complex was subjected to PacBio sequencing followed by primary data analysis (version 2 chemistry and 2.0.1 analysis software) on a PacBio-RS instrument and following manufacturer's recommendations.

For Illumina sequencing, both jumping libraries and 180bp paired fragment libraries were prepared. Jumping libraries were constructed following the approach summarized by Ribeiro et al. (*44*), and paired fragment libraries were constructed using the approach summarized by Fisher et al. (*45*).

To assemble the complete genome of the B594 reference strain, a combination of Illumina paired fragment reads (100x estimated coverage), Illumina paired sheared "jump" reads (118x estimated coverage), and PacBio long reads (48x estimated coverage) were assembled using ALLPATHS-LG version 47300 (*44*). The ALLPATHS-LG assembly was run using default parameters, with the exception of the BIG_MAP option, which was set to "True," to take advantage of longer PacBio sequence data. The resulting ALLPATHS-LG hybrid assembly captured the genome in five contigs, with one contig being mis-assembled in the region of a 16S/23S ribosomal RNA repeat. Error-corrected PacBio reads were previously generated as an intermediate output file during a PacBio-only assembly using HGAP (*46*). These error-corrected reads were aligned to the assembly contigs using BLASR (*47*), and the Illumina fragment and jump read data were each aligned to the assembly contigs using BWA version 0.5.9 (*48*). All aligned BAM files were merged into a single BAM file using SAMtools (*49*), and an ace file was generated using the bam2Ace utility in the Consed package version 23.10 (*50*). This ace file was loaded into the Consed editor (*50*), and the one mis-assembled contig was broken, resulting in a total of six contigs. These six contigs were ordered and oriented using the finished *E. faecalis* V583 genome as a reference (*14*). Four of the contigs corresponded to the B594 chromosome, which measured 3,152,103 bases in length. The remaining two contigs were found to represent two complete and circular plasmids, measuring 70,182 bases and 45,436 bases in length. All chromosome breaks corresponded to the four 16S/23S ribosomal RNA repeats. PacBio error-corrected reads spanning across each entire 16S/23S ribosomal RNA repeat, and which therefore could be anchored uniquely in the genome, were identified and loaded into Consed to close all assembly gaps. Finally, Illumina fragment and jump read data were re-aligned to the three completed B594 contigs (1 chromsomal and 2 plasmids) using BWA (*48*), and these aligned BAM file were

passed through Pilon (*43*), for assembly improvement. Pilon corrected two single base substitution errors and one small (2bp) deletion error.

The remaining 92 draft genomes were sequenced using Illumina and assembled using ALLPATHS (*44*). Assembly statistics and NCBI accession numbers for all sequenced strains are shown in Table S1. The genomes of two previously sequenced and published *E. faecalis* strains, V583 and OG1RF (*14, 51*), were also downloaded from Genbank (assembly accession numbers ASM778v1 and ASM17257v2, respectively) and were included in our phylogenetic analysis, bringing the total number of analyzed genomes to 95.

To further resolve plasmid dynamics in the outbreak strains, seven outbreak strains (B1376, B1532, B1734, B2535, B2949, B3286, and B4969) were sequenced by MinION technology (Oxford Nanopore Technologies, Oxford, UK). 200ng genomic DNA of each strain was used to prepare sequencing libraries using the Rapid Barcoding Kit (Catalog SQK-RBK001), and libraries were pooled and run together on a single flow cell for 48 hours. Bases were called using Albacore, and MinION reads were combined with Illumina paired-end reads and assembled using Unicycler (*52*). These assemblies have been submitted to NCBI under BioProject PRJNA447994.

Genome annotation and phylogenetic analysis

All genomes, including those from Genbank, were annotated using the Broad Institute's prokaryotic annotation pipeline; the *Enterococcus*-specific approach has been described previously (*53*). Briefly, protein-coding genes were predicted with Prodigal (*54*), and were filtered to remove genes with at least 70% overlap to tRNAs or rRNAs. The tRNAs were identified by tRNAscan-SE (*55*), and rRNA genes were predicted using RNAmmer (*56*). Gene product names were assigned based on top BLAST hits against the SwissProt protein database (http://web.expasy.org/docs/swiss-prot_guideline.html; >=70% identity and >=70% query coverage), and protein family profiles were searched against TIGRfam hmmer equivalogs. Additional annotation analyses performed include PFAM (*57*), TIGRfam (*58*), KEGG (*59*), EC (*60*), and TMHMM (*61*).

To establish the genomic diversity of the pre-outbreak and outbreak strains, orthologous genes were identified in all 96 genomes using Synergy2, available at http://sourceforge.net/projects/synergytwo/ (*62*), and trees were constructed using RAxML (*63*). Bootstrapping was performed with RAxML's rapid bootstrapping algorithm, using 1000 bootstrap replicates. The group of 62 most closely related outbreak strains was identified by examining single copy core orthogroups among the 65 sequence type 6 strains in the data set. Removal of strains B3336, B5076, and V583 from this group increased the single copy core genome of the remaining 62 strains, from 2484 orthogroups to 2708 orthogroups. Therefore these 62 strains were considered to be the most closely related outbreak strains.

The presence of virulence (Cytolysin and ESP), bacterial immunity (CRISPR-cas), drug resistance, and plasmid replication genes among the pre-outbreak and outbreak strains was determined using available online tools (VirulenceFinder: https://cge.cbs.dtu.dk/services/VirulenceFinder/; CRISPRfinder: http://crispr.u-psud.fr/Server/; ResFinder: http://cge.cbs.dtu.dk/services/ResFinder/; PlasmidFinder:

https://cge.cbs.dtu.dk/services/PlasmidFinder/). Cytolysin function was verified by testing for hemolysis of human erythrocytes, drug resistances were validated by susceptibility testing, and *rep* gene presence/absence was verified by PCR. In cases of disagreement between results using online tools and either PCR or phenotyping, results from the latter two approaches are reported.

Variant detection and variant filtering

Single nucleotide polymorphism (SNP) and insertion/deletion (indel) variants were detected using Pilon (*43*), using the closed B594 genome as a reference. Variants were canonicalized using Emu (*64*), and a total of 8746 variants among the 62 most closely related outbreak strains were compiled for analysis. In order to distinguish recombination or mobile genetic element movement from *de novo* mutations, the distribution of variants was examined across the B594 genome as well as among outbreak strains. Variants were unevenly distributed across the B594 chromosome, and nearly half of all variants were concentrated in two genomic regions known to be associated with mobile genetic element movement: the *E. faecalis* pathogenicity island (*13*), and a prophage region corresponding to pp4 in V583 (*65*). A total of 4224 variants in these two chromosomal regions were excluded from further analysis. Strains containing these variants are annotated in Fig. S3. Plasmid-borne variants were also unevenly distributed among outbreak strains, due to plasmid variability between strains (Fig. S3). Six strains had an excess (between 368 and 878) of variants on Plasmid #1, which were excluded from further analysis. Finally, 147 indel variants that contained polyN stretches, meaning that they were not fully resolved by Pilon and Emu, were also excluded from further analysis. Application of the above filters resulted in 965 high-confidence variants among all strains, of which 285 were unique (Table S3).

Other comparative genome analyses

The B594 and V583 genomes were compared to one another by first examining variants identified in V583 by Pilon (*43*), and canonicalized with Emu (*64*). Variants suspected to be due to mobile genetic element movement or recombination – using the approach described above – were removed. After filtering, 210 unique and putative *de novo* chromosomal variants remained. Next the B594 and V583 chromosomes were aligned to one another using Mauve (*66*), and larger differences, all residing within mobile genetic elements, were identified. To compare the two B594 plasmids with the three V583 plasmids, sequences were aligned to one another with NUCmer (*67*). A circular plot of all plasmids was generated with lines connecting regions of at least 200bp that share at least 99% nucleotide identity.

To compare the 62 most closely related outbreak strains to one another, a phylogeny was constructed with RAxML (*63*) using 60 SNPs that were shared by at least two strains. Strains with large differences in prophage and pathogenicity island sequences were identified through the variant filtering analyses described above. The plasmid content of each strain was determined by first mapping contigs less than 500Kb of each strain to the two closed plasmids identified in B594. A B594 plasmid was called "present" in the strain if at least 75% of the plasmid was covered by the contigs of the strain. The contigs that did not map to one of the B594 plasmids were further analyzed for the presence of additional *rep* genes, and this information was used to identify strains for additional MinION sequencing as described above. Closed plasmid sequences were generated for the additional four plasmids detected, and the above approach was repeated to determine their distribution among outbreak strains. After this second round comparison no

additional candidate plasmids remained. To compare all six outbreak plasmids to one another, sequences were aligned to one another with MUMmer (67). A circular plot of all plasmids was generated with lines connecting regions of at least 200bp that share 100% nucleotide identity.

Strains and growth conditions for functional assays

For assays using *gntR* wildtype and mutant strains, pairs of outbreak strains were selected that differed in their *gntR* genotypes but were otherwise very closely related to one another. Specifically, for the assays shown in Fig. 4, Fig. S4, Fig. S5, and Fig. S6, paired clones derived from the same frozen cryovial but having different *gntR* genotypes were used. For assays shown in Fig. 5A, Fig. 5C, and Fig. 6C, three different *gntR* wildtype and three different *gntR* mutant outbreak strains (all from different patients) were used. In Fig. 5B and Fig. S7, the MMH594 wildtype strain and corresponding transposon mutants in *gntR*, *ghf65*, or *treB* were used. Transposon mutants were selected from an arrayed transposon library generated previously (2). In Fig. 6B and 6C, three different *pbp4* wildtype and three different *pbp4* mutant strains (all from different patients) were used. In Fig. 6D and Fig. S10, an isogenic pair of MMH594 wildtype and *pbp4* -82delT mutant (which was selected *in vitro* for resistance to meropenem) strains were used. Unless otherwise noted, all strains were grown in BHI media at 37^OC shaking at 220rpm. In Fig. S7, strains were grown in a chemically defined media that has been previously described (68), containing either 0.5% (w:v) glucose, trehalose, or kojibiose.

Construction of markerless deletion mutants

E. faecalis strains bearing markerless deletions of the *ghf65/pgmB* genes or the *cydABDC* operon were generated using the pLT06 vector and following previously published methods (69). Primers used to generate the two flanking regions for each deletion mutant were: *ghf65/pgmB* Flank1_F: 5'-TGCGCTCCACAGGAATTTCTT-3' Flank1_R: 5'-CCCAGGCACGTAGCCATAAT-3' Flank2_F: 5'-TCGGCCAGCCAACCCTTAA-3' Flank2_R: 5'-CGATAATAAAGATTGTGGAACG-3', and *cydABDC* Flank1_F: 5'-GCAAATTATTACGCCCCGCT-3' Flank1_R: 5'- CCGTCATCTGGATTACCCACC-3' Flank2_F: 5'- GGAAAACTGTTGTCATCGCA-3' Flank2_R: 5'-TCAAGAGCTTTTCGCGATTG-3'. Briefly, flanking regions were amplified by PCR, joined either with ligation or SOEing PCR, and the insert was digested and ligated into the pLT06 vector. After propagation and amplification in *E. coli* EC1000 cells, vectors were transformed into either an outbreak *E. faecalis* strain with a *gntR* mutant background (to create the *ghf65/pgmB* knockout strain), or MMH594 to create the *cydABDC* knockout strain. Transformed strains were passaged at 30^OC for two days, then were switched to 42^OC to select for integrants. Integrants were cured by passaging again at 30^OC in the absence of positive selective pressure, and then strains were plated onto media containing p-chlorophenylalanine (for negative selection), and were grown at 37^OC. Resulting colonies were screened with PCR to identify a clone containing the mutant allele of interest. The *ghf65/pgmB* knockout strain was complemented with either gene individually by cloning into the pAT28 shuttle vector (70). Primers used to amplify the *ghf65* open reading frame and native promoter were F: 5'-GCCGATCCTCCTCTACC-3' and R: 5'-GGTTCGCTCCTTTATTGATAATGTAC-3'. Because *pgmB* does not appear to have its own promoter, the open reading frame was amplified and was ligated to the native promoter upstream of *ghf65* using SOEing PCR. Approximately 500bp of the *ghf65* coding sequence was also included to preserve the native gene context.

Primers used for the amplification of *pgmB* were F: 5'-GGAGCGAACCACAATGACG-3' and R: 5'-TTAGCGATTGAGCAGTGC-3', and primers used for the amplification of the promoter region were F: 5'-GCCGATCCTCCTCTACC-3' and R: 5'-TCGTCATCTCAGGTGTCGTG-3'.

RNA sequencing and quantitative real-time PCR (qPCR)

RNA was prepared from *gntR* and *pbp4* wildtype and mutant cultures grown to late-log phase in BHI broth. Cells were added to two volumes of RNAProtect Bacteria Reagent from Qiagen (Valencia, CA; Catalog 76506), incubated for five minutes at room temperature, and pelleted at 8,000 rpm for 10 minutes. The supernatant was discarded and cells were stored at -20^OC until extraction of RNA. RNA was extracted using a Qiagen RNeasy Kit (Catalog 74104) following the protocol for RNA isolation from Gram-positive bacteria. Briefly, cells were incubated in 100uL of 15mg/mL lysozyme for 30 minutes at room temperature prior to addition of buffer RLT, and Lysing Matrix B tubes from MPBio (Santa Ana, CA; Catalog 6911-050) were used to lyse cells in a MPBio FastPrep 24. Total RNA was treated with DNase using the Turbo DNase-free Kit from Thermo Fischer Scientific (Waltham, MA; Catalog AM1907), and RNA quality was checked on an Agilent 2100 Bioanalyzer (Santa Clara, CA).

For RNA sequencing, ribosomal RNA was depleted using the RiboMinus Bacteria Kit and Concentration Module from Thermo Fischer Scientific (Catalog K1550-04, K1550-05), and cDNA synthesis and sequencing libraries were prepared with the ScriptSeqv2 Kit from Illumina (San Diego, CA; Catalog SSV21124). Libraries were sequenced with 2x100bp paired end reads on an Illumina HiSeq machine, and data were analyzed using CLC Genomics Workbench v8, using default parameters and the closed B594 chromosome as a reference. Differential gene expression was determined by comparing reads per kilobase per million mapped reads (RPKM) from three independent replicates of each genotype. Raw sequencing reads were submitted to the NCBI Sequence Read Archive (SRA) under accession number SRP136460.

For qPCR, cDNA was synthesized using the SuperScript III First-strand Synthesis Kit from Invitrogen (Carlsbad, CA; Catalog 18080-051), and quantitative real-time PCR was conducted using a Qiagen Rotor-Gene. Expression of *penicillin-binding protein 4* (*pbp4*; gene ID EF2476 in V583) was quantified relative to *glucose 6-phosphate dehydrogenase* (*gdh*; gene ID EF1004 in V583) using the following primers: 5'-TTCTTGGTGTTTCTGCCTTG-3' and 5'-TCTTCGCTTCGGCTAATTCT-3' for *pbp4*, and 5'-ATTTGCAGCCTATCGTGATG-3' and 5'-GCCAGACCAACGGAAATTAT-3' for *gdh*. Ct values were normalized based on standard curves for each primer pair, and *pbp4* fold expression was calculated relative to *gdh* expression for at least three replicate samples each of wildtype and mutant bacterial strains.

Electron microscopy and image analysis

gntR wildtype and mutant strains were grown overnight in BHI media, and cells were fixed in 2.5% glutaraldehyde, 1.25% paraformaldehyde, and 0.03% picric acid in 0.1 M sodium cacodylate buffer (pH 7.4). Cell pellets were fixed for at least two hours at room temperature. For scanning electron microscopy, cells were deposited onto poly-lysine coated coverslips and dried completely. Half-strength Karnovsky's fixative in 0.1M PO_4 buffer was added for 15-20 minutes, then coverslips were rinsed with 1x PBS and dehydrated with graded ethanols (50%, 70%, 85%, 95%, 100%) at 10-minute intervals. Samples were then dried with a Tousimis Semi

Automatic Critical Point Dryer, and a Gatan Ion Beam coater was used to coat the samples with chromium, before imaging on a JEOL 7401 Field Emission scanning electron microscope. Images were collected at 10,000x magnification.

For transmission electron microscopy, fixed pellets were washed in 0.1M cacodylate buffer and post-fixed with 1% osmium tetroxide (OsO_4)/1.5% potassium ferrocyanide ($KFeCN_6$) for 1 hour, washed twice in water, washed once in maleate buffer (MB), and were washed and then incubated in 1% uranyl acetate in MB for 1 hour followed by two washes in water and subsequent dehydration in grades of alcohol (10min each; 50%, 70%, 90%, 2x10min 100%). The samples were then put into propylene oxide for 1 hour and infiltrated overnight in a 1:1 mixture of propylene oxide and TAAB Epon from Marivac Canada, Inc. (St. Laurent, Canada). The following day the samples were embedded in TAAB Epon and polymerized at 60^OC for 48 hours. Ultrathin sections (about 60nm) were cut on a Reichert Ultracut-S microtome, picked up onto copper grids stained with lead citrate, and examined in a JEOL 1200EX Transmission electron microscope. Images were recorded with an AMT 2k CCD camera.

For image analysis of transmission electron micrographs, micrographs collected at 2000x or 3000x magnification were first cropped to remove white space. Cropped images were corrected for uneven background intensity in the image using pseudo flat field correction. A Gaussian blur was created for each image, and Sigma (the radius that was used to blur the image) was set at 400 for 2000x images and 200 for 3000x images. The cropped original image was divided by the signal from the blurred map to correct the background. Corrected images were processed using MatLab from MathWorks (Natick, MA). Images were thresholded based on intensity, and pixels greater than 1.1x the mean intensity were removed. Very small objects (fewer than 6 pixels) were also removed. For each object in the thresholded image, the area, intensity, and aspect ratio were calculated and compared across strains.

Monosaccharide composition analysis of surface-associated polysaccharides

Surface-associated polysaccharides (capsular polysaccharide, epa polysaccharide, wall teichoic acid, and lipoteichoic acid) were extracted from *gntR* wildtype and mutant strains following a previously described approach (*69*). Precipitated polysaccharide pellets were submitted for monosaccharide composition analysis to the Complex Carbohydrate Resource Center at the University of Georgia (Athens, GA). Glycosyl composition analysis was performed by combined gas chromatography/mass spectrometry (GC/MS) of the per-O-trimethylsilyl (TMS) derivatives of the monosaccharide methyl glycosides produced from each sample by acidic methanolysis as described previously (*71*). Briefly, the samples (100-300 ug) were heated with methanolic HCl in sealed screw-top glass test tubes for 16 hours at 80^OC. After cooling and removal of the solvent under a stream of nitrogen, the samples were treated with a mixture of methanol, pyridine, and acetic anhydride for 30 minutes. The solvents were evaporated, and the samples were derivatized with Tri-Sil® (Pierce) at 80^OC for 30 minutes. GC/MS analysis of the TMS methyl glycosides was performed on an Agilent 7890A GC interfaced to a 5975C MSD, using a Supelco Equity-1 fused silica capillary column (30 m × 0.25 mm).

Lipoteichoic acid extraction and analysis

Lipoteichoic acid (LTA) was extracted and purified from one-liter cultures of *gntR* wildtype or mutant strains using hydrophobic interaction chromatography (HIC) by adapting a previously described protocol (*27*). Briefly, overnight cultures were spun down and washed in 100mL 1xPBS, and were resuspended in 10mL 0.1M sodium citrate (pH4.7). Bacteria were lysed by bead beating in Lysing Matrix B tubes from MPBio (Santa Ana, CA; Catalog 6911-050), and were lysed in a MPBio FastPrep 24. Following lysis, tubes were spun down at 200g for one minute to pellet beads, and lysates were pooled for each strain. 10mL cell lysate was mixed with 10mL 1-butanol and incubated for 30 minutes with end-over-end rotation. The mixture was then spun down at 14,000g for 10 minutes, the lower aqueous phase was transferred to a new tube, and 8mL 1-butanol was added to the top phase for a second extraction for 30 minutes with end-over-end rotation. The mixture was again spun down at 14,000g for 10 minutes, the lower aqueous phases were pooled, and the volume was adjusted to 10mL using ammonium acetate (0.1M final concentration), 1-propanol (15% final) and water. A glass drip chromatography column was packed with Octyl-Sepharose 4 Fast Flow from GE (Boston, MA; Catalog 17094604) and was washed extensively with running buffer (0.1M ammonium acetate/15% 1-propanol), before the lysate was applied to the column. The column was washed with 30-40mL of running buffer, and then LTA was eluted with a step gradient of 0.1M ammonium acetate containing increasing concentrations (30%, 45%, 60%) of 1-propanol. Fractions of 1.5mL were collected, and fractions containing LTA were identified by detection of inorganic phosphate, as described previously (*72*). LTA-containing fractions were pooled and dialyzed overnight against water, and samples were concentrated using a speed-vac. Total extracted LTA for each strain was quantified again in the pooled fractions, and was normalized to total protein present in the lysate applied to the HIC column, as measured using the Bradford assay reagent from VWR (Radnor, PA; Catalog 97065-020).

Nuclear magnetic resonance spectroscopy was performed on the LTA extracted from *gntR* wildtype and mutant strains, following previously published methods (*27*). LTA dissolved in water was exchanged with D_2O by repeated lyophilization, and one-dimensional ^{1}H-NMR scans were collected at 27^OC with a Bruker Avance II 600MHz Bio-molecular NMR System (Billerica, MA). Chemical shifts reported previously for the $-CH_3$ fatty acid protons and the protons within the side chain kojibiose residues were used to identify peaks of interest (*27*), and these were integrated and compared to one another using TopSpin software.

Killing assays and drug susceptibility testing

Killing assays with ampicillin were performed by first diluting overnight cultures of wildtype and mutant bacteria 1:100 into BHI broth and growing for three hours at 37^OC shaking at 220rpm. After three hours, CFU/mL in each culture was determined by serial dilution and track plating onto BHI agar, then ampicillin was added to a final concentration of 256ug/mL and cultures were incubated for 24 hours at 37^OC shaking at 220rpm. After 24 hours, CFU/mL were determined again, and survival was calculated as the percentage of the starting CFU/mL. Lysozyme killing assays were performed by spinning down 500uL of stationary-phase cultures grown in BHI broth and then resuspending the bacterial pellet in 500uL TE buffer containing 10mg/mL lysozyme. CFU/mL were determined before lysozyme addition and after 30 minutes of incubation at 37^OC, and survival was calculated as the percentage of starting CFU/mL. Autolysis assays were performed by diluting overnight cultures 1:100 into BHI broth and growing for three hours at 37^OC shaking at 220rpm. After three hours, cells were spun down and

washed once with 5mL cold water, and were resuspended in 50mM Tris (pH7.5) with 0.1% Triton X-100. Cells were aliquoted into a 96-well plate, and OD600 values were collected every 15 minutes using a Synergy2 Biotek plate reader (Winooski, VT) and Gen5 software. Lysis was calculated by dividing the OD600 at each time point by the starting OD600 and multiplying by 100.

To determine IC_{50} values, wildtype, *gntR* mutant, and *pbp4* mutant strains were inoculated into Mueller Hinton II media containing serial dilutions of ampicillin, ceftriaxone, imipenem, and vancomycin. Growth was measured as optical density (OD_{600}) after 24 hours in the presences of varying drug concentrations, and OD_{600} values were used to calculate IC_{50}s by fitting dose-response log-logistic curves using GraphPad Prism (La Jolla, CA).

Whole blood killing assays

Whole blood killing assays were performed as described previously (*18*). Briefly, wildtype and mutant bacteria grown to stationary phase in BHI broth were mixed 1:1, and 10^5 CFU in 10uL were added to 90uL fresh whole human blood purchased from Research Blood Components (Boston, MA). Blood from six different de-identified donors was used. The bacterial mixture alone was serially diluted and track plated on BHI agar and grown overnight at 37^OC. Blood-bacteria mixtures were incubated at 37^OC for six hours with no agitation, and then the mixture was serially diluted and track plated onto Todd Hewitt agar containing 0.5% yeast extract and 0.4% sheep blood (THYB). For the *gntR* wildtype/mutant mixture, the ratio of wild-type to mutant bacteria at the beginning of the assay and after six hours was determined by plating onto THYB with and without 10ug/mL tetracycline. For the *cydABDC* operon wildtype/mutant mixture, individual colonies were genotyped by PCR using the following primers: 5'-AATGACAACCCAATCCCCAT-3' and 5'-GATGGAACGAACCAATAGCG-3'. PCR products were run on a 1% agarose gel and stained with ethidium bromide. Mutant colonies yielded a 4.3Kb product, while wildtype colonies had a 9.7Kb product. For the *pbp4* wildtype/mutant mixture, individual colonies were genotyped by PCR and Sanger sequencing. The region upstream of the *pbp4* gene was amplified with the following primers: 5'-CAATAACCTCTAGCCATTGATCG-3' and 5'- TCCACGTTTGGCATTATCTACTT-3' and was submitted for Sanger sequencing to Genewiz, Inc. (South Plainfield, NJ).

Mouse abscess infections

Mouse abscess infections were performed as previously described (*33*). All animal studies were approved by the Institutional Animal Care and Use Committee at Massachusetts General Hospital, as well as the Office of Laboratory Animal Welfare. Studies followed the guidelines of the Association for Assessment and Accreditation of Laboratory Animal Care. Swiss Webster male mice aged 5 to 7 weeks were purchased from Charles River Laboratories (Wilmington, MA), and were housed in the biosafety level 2 animal facility located at Massachusetts General Hospital (Boston, MA). Wildtype and mutant bacteria were grown overnight in BHI broth, then were diluted to OD600=0.8 in 1xPBS. The mixture was diluted 1:20 into 1xPBS and then mixed with an equal volume of autoclaved Cytodex-1 microcarrier beads (1g in 50ml PBB) (Sigma-Aldrich, St. Louis, MO) in 1x PBS. 0.2ml of the mixture of cells and beads was then injected subcutaneously into each shaved flank of each mouse anesthetized with ketamine and xylazine. The inoculum for each abscess typically contained 1-3x10^6 bacteria. Twenty-four hours after

infection, mice were euthanized and the subcutaneous abscesses were harvested and homogenized in PBS. Before and after infection, bacterial mixtures were serially diluted and track plated on BHI agar, and individual colonies were genotyped by qPCR with high-resolution melting (HRM) genotyping, or by PCR and Sanger sequencing. The following HRM primers were used: 5'-AAGAAATTCCTGTGGAGCGCAA-3', 5'-CGACTTCCCCTTCAATCTCCCG-3', 5'-ACAAGGAGTTACAACAAACGCAACA-3', 5'-CAACCAGTCAACTGAGCCAAGTT-3'. For PCR and Sanger sequencing, the following primers were used: 5'-GTCGTCGTTAGTTGGTTCGTTGCG-3' and 5'-CCGTCAATTTTCATTTAATGACAGCCG-3'.
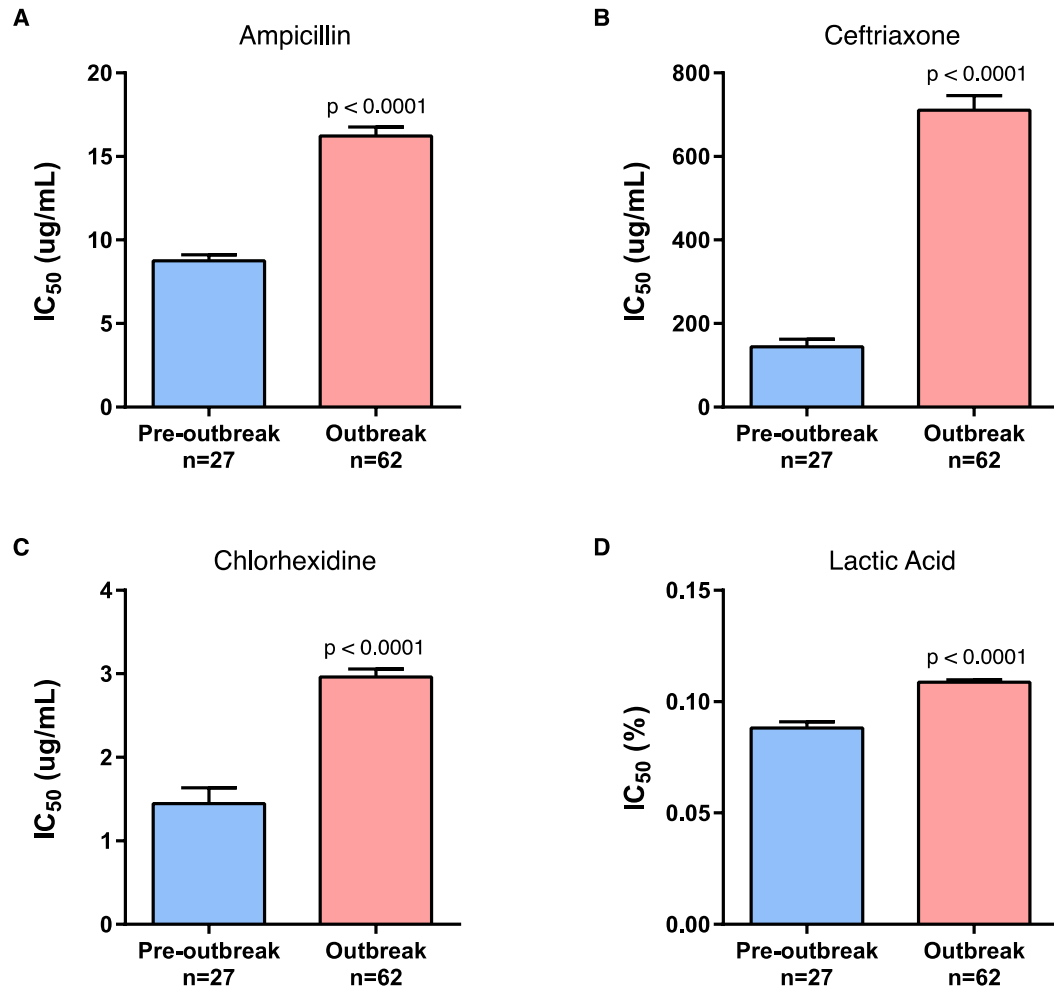
Fig. S1. Phenotypic differences between pre-outbreak and outbreak *E. faecalis* strains. Summary of 50% inhibitory concentration (IC_{50}) values of Ampicillin (**A**), Ceftriaxone (**B**), Chlorhexidine (**C**), and Lactic Acid (**D**) measured in 27 pre-outbreak and 62 outbreak strains. Strains belonging to each group are indicated in Fig. 1. Bar charts show mean values with error bars indicating standard deviation, and p-values indicate results from two-tailed t-tests.
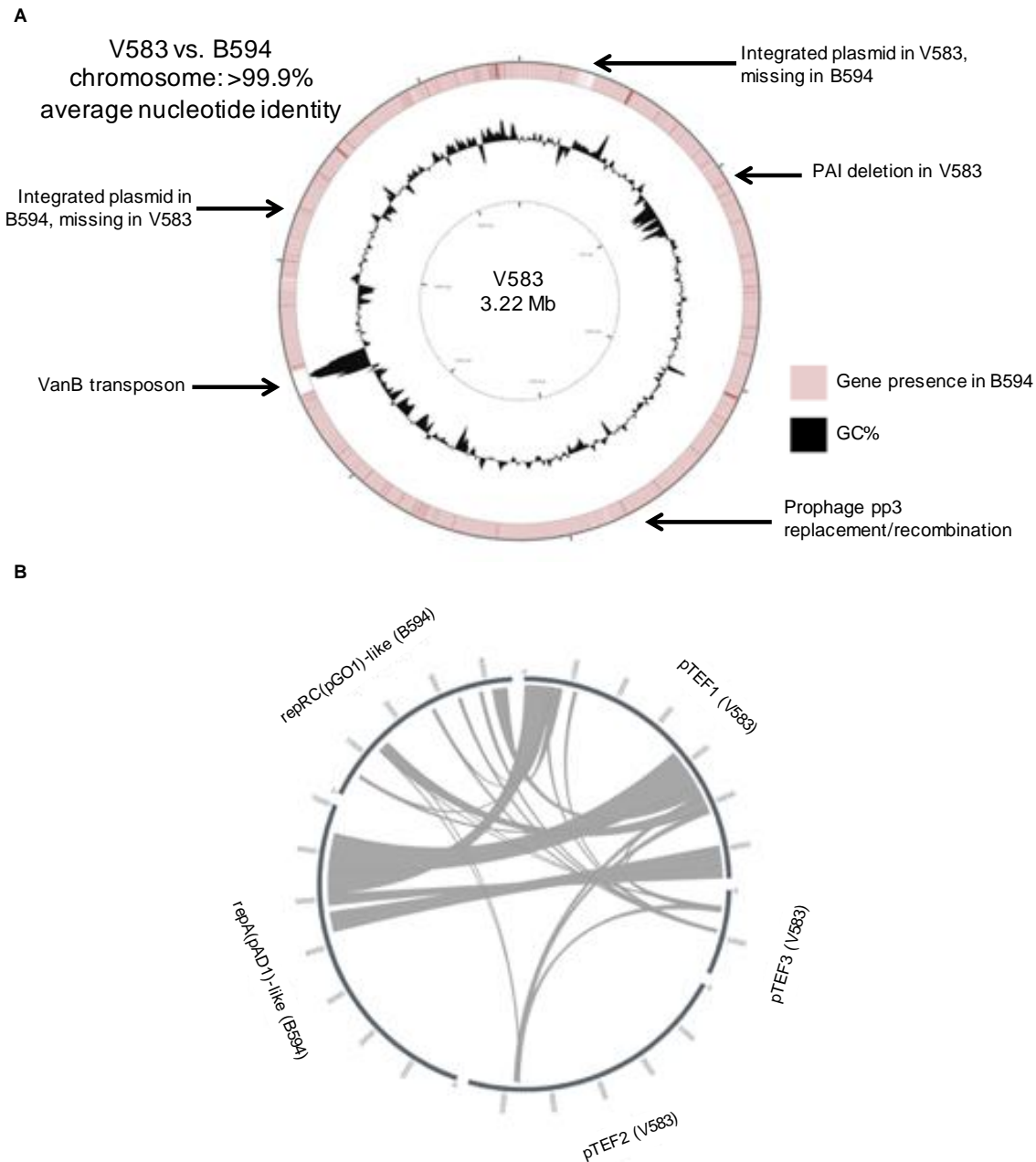
A

V583 vs. B594 chromosome: >99.9% average nucleotide identity

Integrated plasmid in V583, missing in B594

PAI deletion in V583

Integrated plasmid in B594, missing in V583

V583
3.22 Mb

VanB transposon

Gene presence in B594

GC%

Prophage pp3 replacement/recombination

B

repRC(pGO1)-like (B594)

pTEF1 (V583)

repA(pAD1)-like (B594)

pTEF3 (V583)

pTEF2 (V583)

Fig. S2. Comparison of *E. faecalis* B594 and V583 strain genomes. (**A**) Differences between the B594 and V583 chromosomes, as determined by Mauve alignment. The two chromosomes differs by 210 variants over 3.04Mb of shared sequence, resulting in >99.9% average nucleotide identity. The circular plot shows the V583 chromosome, with mobile element differences from B594 indicated with black arrows. Pink shading indicates genes in V583 that are found on the B594 chromosome using BLAST. (**B**) Comparison of plasmids between B594 and V583. The two B594 plasmids and three V583 plasmids were compared to one another using NUCmer and plotted using Circos. Lines connect regions >200bp that are >99% identical.
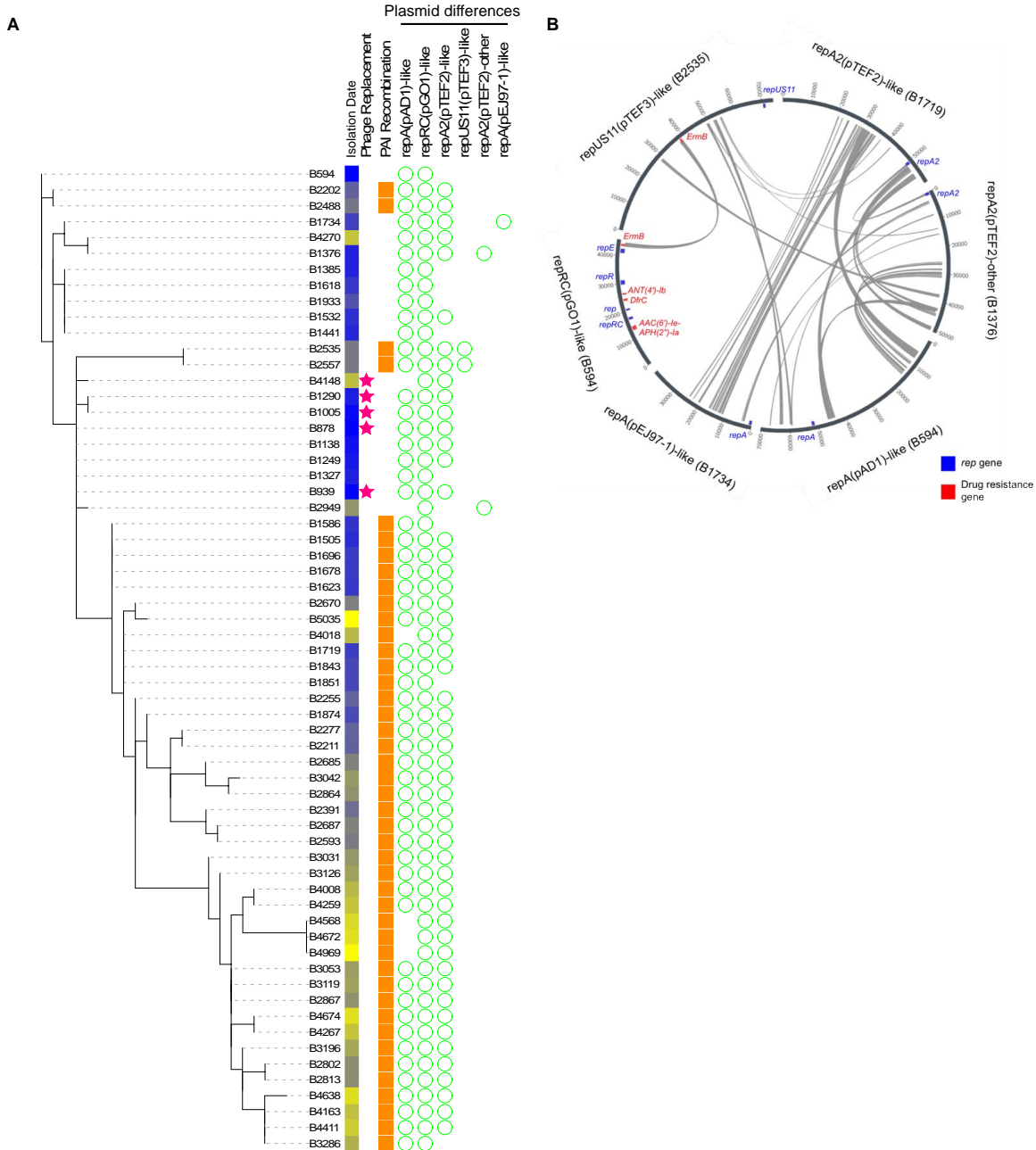
Fig. S3. Phylogeny of 62 *E. faecalis* outbreak strains. (A) Phylogeny was constructed from 60 SNPs found in >1 strain using RAxML. Colored boxes show the date of isolation of each strain (blue = earlier; yellow = later), and colored shapes show mobile genetic element differences between strains. These include an approximately 32Kb prophage recombination/replacement in five strains (pink stars), a 2.2Kb recombination within the pathogenicity island in 44 strains (oranges squares), and six plasmids (green rings), five of which were variably present between strains. (B) Comparison of six distinct plasmids detected among outbreak strains. Plasmids were compared to one another using MUMmer and plotted using Circos. Lines connect regions >200bp that are 100% identical. Plasmids are named according to their rep gene (associated plasmid) and the strain in which the depicted plasmid is found. Blue boxes and labels show the location of rep genes, and red boxes and labels show predicted drug resistance genes.

A
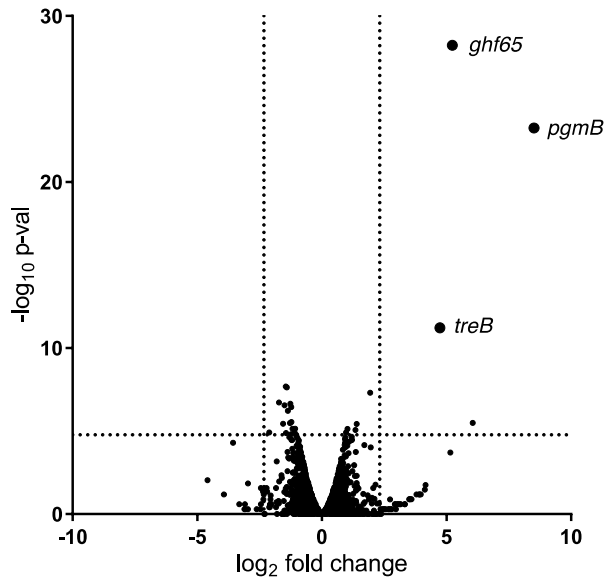
B

Gene ID (B594)	Gene product	Fold Change MUT	Bonferroni p-val
SAW_02999	Glycosyl Hydrolase (ghf65)	37.77	1.79E-25
SAW_03000	Beta-phosphoglucomutase (pgmB)	365.39	1.68E-20
SAW_02140	PTS system, trehalose-specific IIBC (treB)	26.60	1.83E-08
SAW_00341	Phage protein	-2.73	6.35E-05
SAW_02792	Cold-shock protein CspA	-2.64	7.11E-05
SAW_02843	HlyD family secretion protein	3.83	1.48E-04
SAW_01287	Hypothetical protein	-3.29	0.0006
SAW_00333	Phage scaffold protein	-2.39	0.0007
SAW_01299	Hypothetical protein	-2.82	0.0008
SAW_00337	Phage protein	-2.35	0.0011
SAW_00348	Phage holin	-2.58	0.0018
SAW_00339	Phage protein	-2.33	0.0087
SAW_01225	Hypothetical protein	66.50	0.0097
SAW_00328	Phage protein	-2.43	0.0101
SAW_00349	Phage endolysin	-2.94	0.0110
SAW_02549	D-alanyl-lipoteichoic acid biosynthesis protein DltB	2.62	0.0114
SAW_02793	Hypothetical protein	-2.10	0.0216
SAW_02762	Hypothetical protein	-2.27	0.0221
SAW_01549	NADH oxidase Npx	2.04	0.0223
SAW_01984	ABC transporter permease YvcS	2.55	0.0258
SAW_02014	Hypothetical protein	-4.33	0.0362
SAW_02296	PTS system, glucose-specific IIA	-2.14	0.0364
SAW_00188	Elongation factor Tu	1.96	0.0369
SAW_00656	Hypothetical protein	-2.71	0.0397
SAW_00336	Phage adapter protein	-2.35	0.0483

Fig. S4. Summary of gene expression differences between *gntR* wild-type and mutant *E. faecalis* strains measured by RNA sequencing. (**A**) Volcano plot showing p-value versus fold change for 3049 genes in three *gntR* mutant strain replicates compared to three wildtype replicates. Vertical lines indicate five-fold change in expression, and horizontal lines show the p-value cutoff for significance after correction for multiple testing. Genes shown in Figure 4A are labeled. (**B**) Summary of all differentially expressed genes between *gntR* wildtype and mutant strains, regardless of fold change. Genes with Bonferroni-corrected p-values <0.5 are shown.
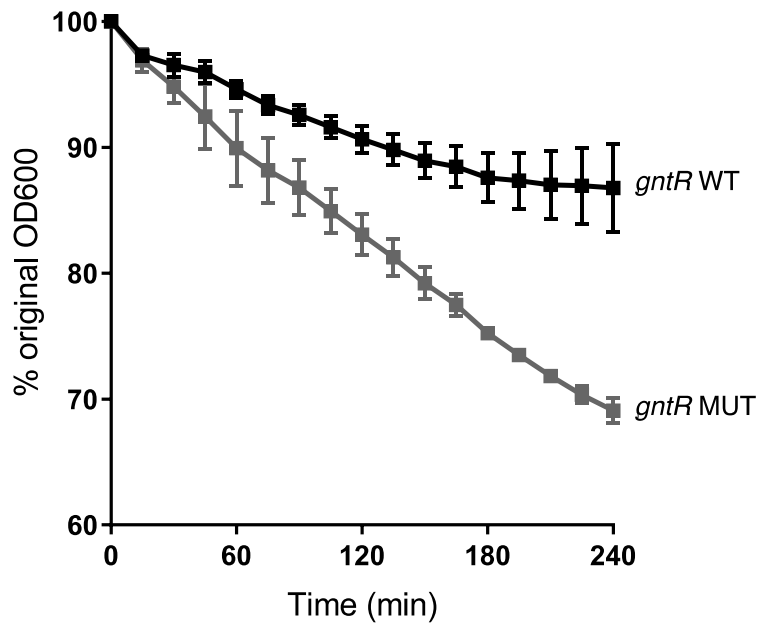
Fig. S5. Difference in autolysis between *gntR* wild-type and mutant strains. Wildtype (WT) or mutant (MUT) cells were incubated with 0.1% Triton X-100, and optical density (OD600) was measured over time. Lysis is shown as the percentage of the starting OD600. Mean +/- standard deviation of triplicate values collected from two biological replicates are shown.
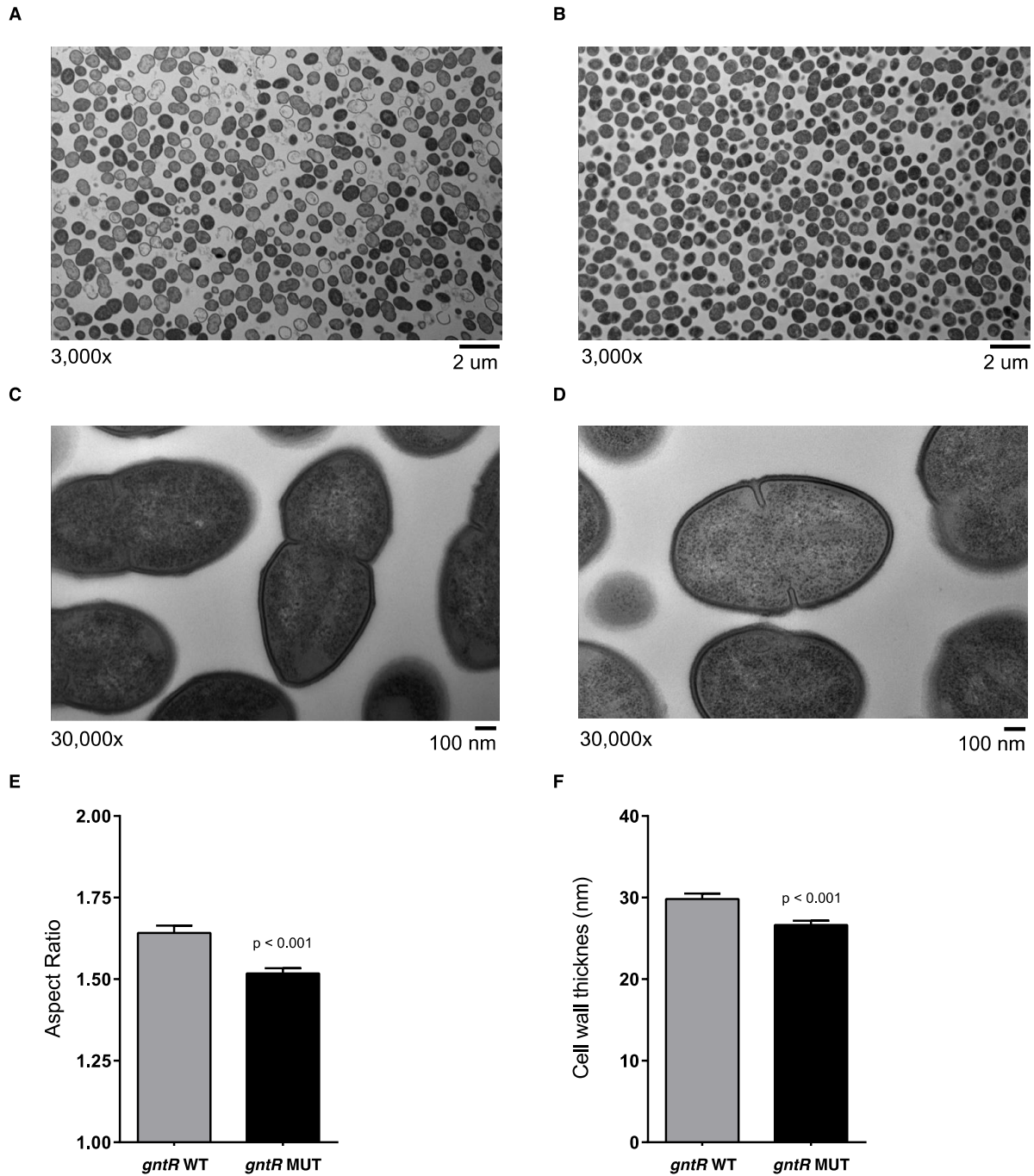
Fig. S6. Morphological differences between *gntR* wild-type and mutant strains. Transmission electron micrographs of (**A, C**) *gntR* wildtype (WT) and (**B, D**) mutant (MUT) stationary phase cultures grown in brain heart infusion media. Magnifications and scale bars are shown below each micrograph. (**E**) Cellular aspect ratios (length/width) calculated from TEM images of GntR WT and MUT cultures. At least 2000 cells of each genotype were analyzed and images were processed using MatLab. (**F**) Cell wall thickness of *gntR* WT and MUT cells. Measurements were made on TEM images of at least 30 cells of each genotype. In panels (E) and (F) bar charts show mean values with error bars indicating standard deviations, and p-values indicate results from two-tailed t-tests.
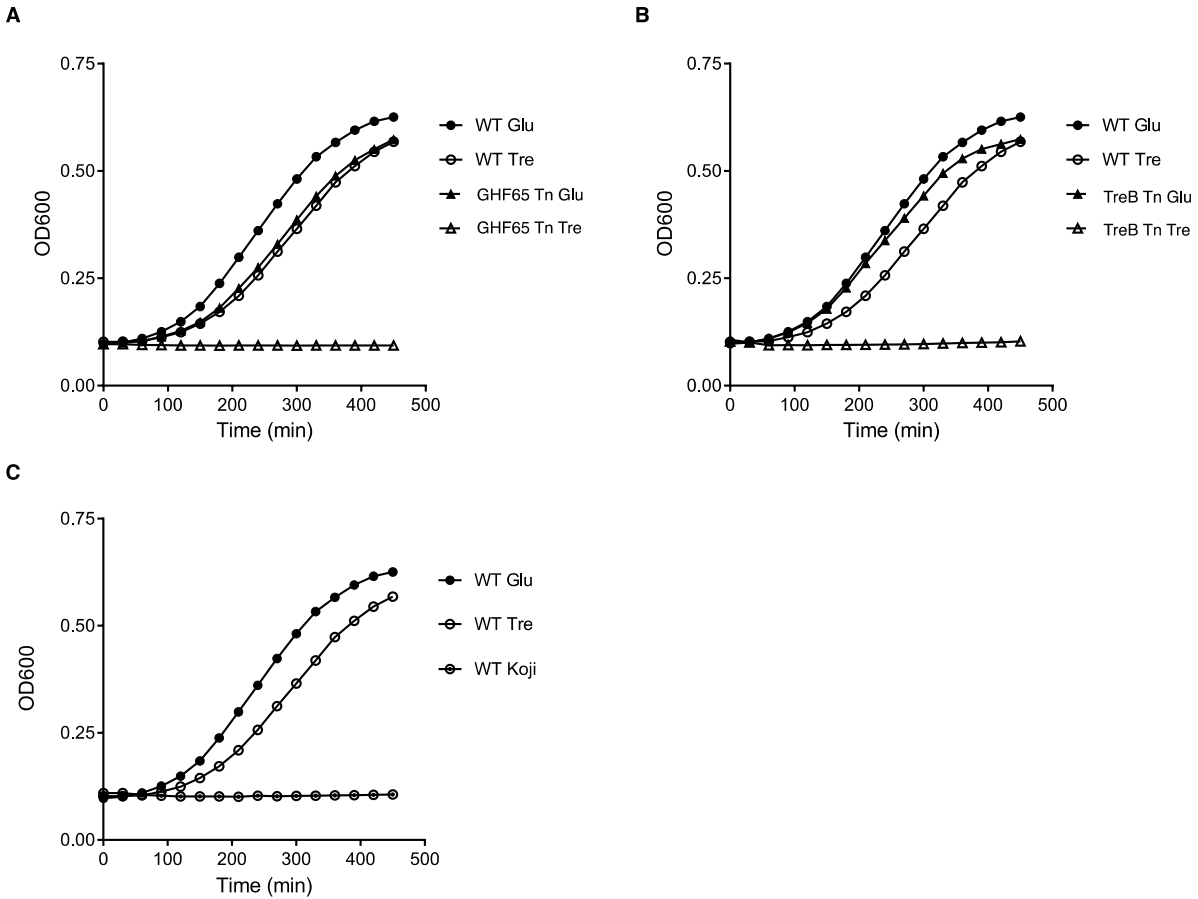
Fig. S7. Growth curves of MMH594 wild-type and mutant strains in the presence of different sugars. (**A**) Comparison of the wildtype (WT) strain with an isogenic derivative strain containing a transposon insertion within the glycoside hydrolase 65 family enzyme (GHF65 Tn) that is expressed in *gntR* mutants. Strains were grown in complete defined media containing 0.5% glucose (Glu) or trehalose (Tre) as the sole carbon source. (**B**) Comparison of the WT strain with an isogenic derivate strain containing a transposon insertion within the phosphotransferase (TreB Tn) that is expressed in *gntR* mutants. (**C**) Growth curves of the WT strain with 0.5% Glu, Tre, or kojibiose (Koji) as the sole carbon source. In all panels, optical density (OD600) was measured every 30 minutes, and curves show the average of four replicates. Error bars (standard deviations) are too small to be visualized on the plots.
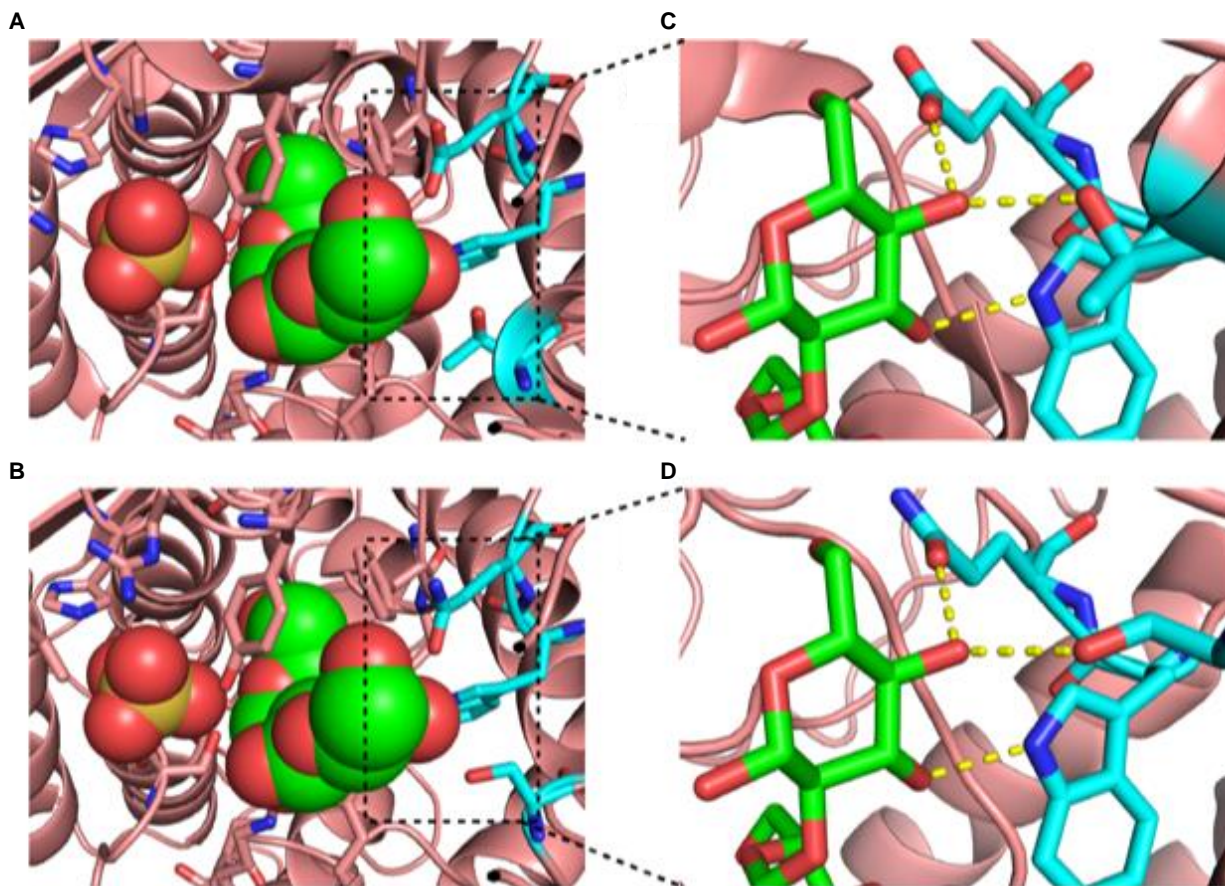
Fig. S8. Active site modeling of the GHF65 enzyme. (A) The previously-solved crystal structure of the *C. saccharolyticus* kojibiose phosphorylase (PDB IDs 3wiq) (*25*), showing substrates phosphate (gold) and kojibiose (Glc(α1→α2)Glc) (green) in spheres. **(B)** Comparative model of the *E. faecalis* GH65 enzyme built from the template in (A) using SWISS-MODEL (*30)*, showing conservation of the active site. **(C)** Previous mutagenesis studies implicated positions 391/392/417 (*cyan*) of the *C. saccharolyticus* enzyme in determining substrate specificity (*29*); the crystal structure explains this observation by showing that each of these residues (Trp/Glu/Thr) make hydrogen bonds to the substrate at the glucose furthest from the phosphate (yellow). Replacement of kojibiose with trehalose (Glc(α1↔α1)Glc) requires repositioning the anomeric carbon of this glucose unit to participate in a glycosidic bond to the preceding glucose unit, corresponding to a counterclockwise rotation of this sugar (in the perspective shown). This would alter the stereochemistry at each of the positions shown involved in hydrogen bonding to the enzyme, disrupting these interactions and suggesting that different amino acids would be required at these positions for recognition of trehalose. Indeed, mutagenesis has shown that changing the identity of the residues shown in cyan can alter the substrate specificity towards trehalose (or other disaccharides) instead of kojibiose (*29*). **(D)** The *E. faecalis* GH65 enzyme harbors Trp/Gln/Ser at the corresponding positions, structurally mimicking the Trp/Glu/Thr triad in the *C. saccharolyticus* kojibiose phosphorylase and strongly supporting its activity towards kojibiose.
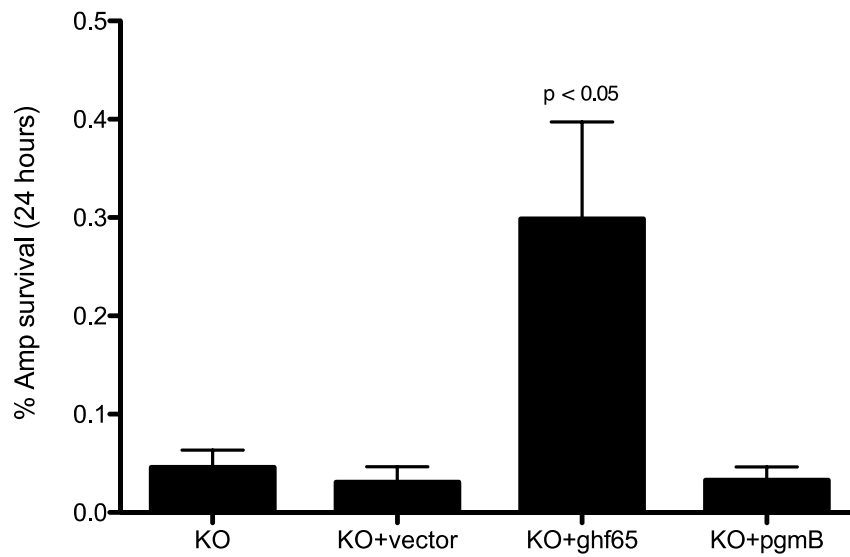
Fig. S9. Increased resistance to ampicillin killing in *gntR* mutants due to the constitutive expression of the GHF65 enzyme. Strains were treated for 24 hours with a lethal dose (10X WT MIC) of ampicillin and CFU/mL were determined at the beginning and end of the assay. Survival was calculated as a percentage of the starting CFU/mL. KO=*ghf65/pgmB* knockout strain. Mean values are plotted with error bars showing the standard deviation among triplicate experiments. p-value indicates the result of a two-tailed t-test comparing KO and KO+*ghf65* strains; all other comparisons are not statistically significant.
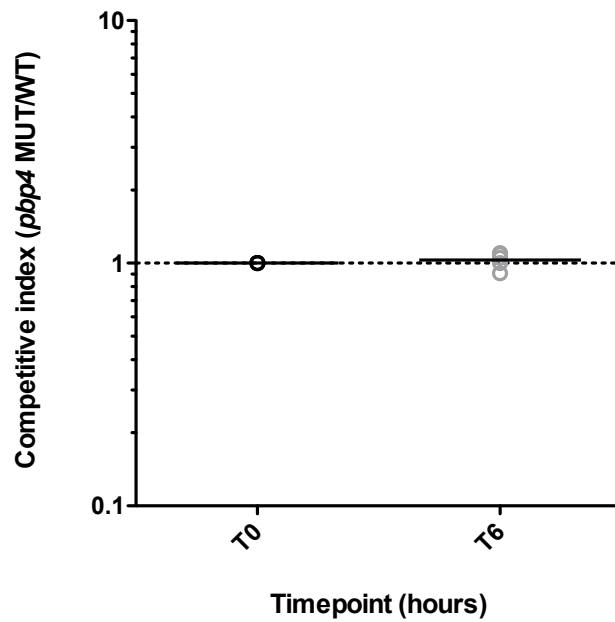
Fig. S10. Killing assay in whole human blood with *pbp4* wild-type and mutant strains. Strains were mixed 1:1 and were incubated with fresh whole human blood from six different donors for six hours. Competitive index was calculated as the ratio of MUT/WT cells, and was determined by selective plating. The difference between competitive index at T0 vs. T6 is not statistically significant.
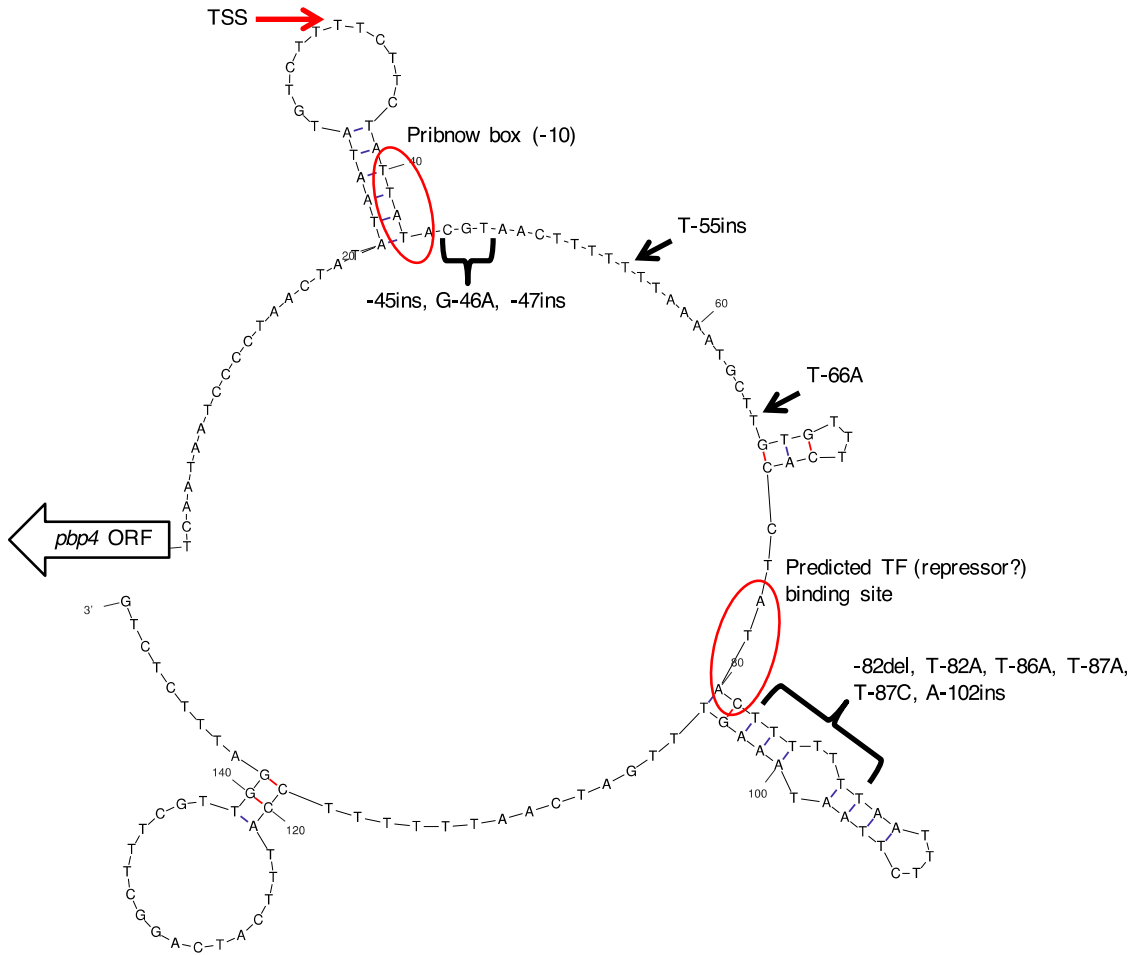
Fig. S11. Predicted secondary structure of the region upstream of *pbp4* and location of mutations identified in in vitro–selected meropenem-resistant strains. The predicted folding of the *pbp4* upstream sequence was generated with mFold (http://unafold.rna.albany.edu/?q=mfold), and relevant transcriptional features are marked in red. Black brackets and arrow indicate the locations of mutations that were identified among *in vitro* meropenem-resistant strains. TSS = transcription start site. TF = transcription factor.